

4
5 **The importance of coupling agent on tensile and thermomechanical performance of**
6 **annealed composites based on poly(lactic acid)/poly(methyl methacrylate) matrix**
7 **and sisal fiber bundles**

8
9 **Abstract**

10 The main aim of this work is to study the importance of the coupling agent on tensile and
11 thermomechanical performance of annealed composites based on poly(lactic
12 acid)/poly(methyl methacrylate) matrix and sisal fiber bundles. As coupling agent
13 poly(styrene-co-glycidyl methacrylate) copolymer was used. Results obtained in the
14 current study suggested that the presence of the copolymer is crucial to form a strong
15 adhesion between the fibers and polymeric matrix and consequently to improve both
16 thermomechanical performance and tensile properties after annealing process. It must
17 highlight that the estimated heat deflection temperature (HDT) of annealed composite
18 with 40 wt% of fiber increased around 40 °C respect to respect to commercial neat PLA.

19
20 **Keywords**

21 Sisal fibers; Polymer-matrix composites; Mechanical properties; Thermomechanical
22 properties

23
24 **1. Introduction**

25 In the last decades, the research in sisal fiber-reinforced composite caught the interest of
26 researchers due to its properties and environmental benefits. Different polymer matrices

27 have been used for sisal fiber composite preparation (Arbelaiz et al. 2020; Bosquetti et
28 al. 2019; Zhao, Sun, and Tang 2020; Zhu, Hao, and Zhang 2020). In the recent years,
29 the development of composites based on biopolymers such as poly(lactic acid) (PLA)
30 has gained a great interest (Orue et al. 2015, 2016, 2020; Orue, Eceiza, and Arbelaiz
31 2018). One of the most studied approaches to overcome PLAs poor impact strength and
32 low heat distortion temperature (Auras, Harte, and Selke, 2004; Kale et al. 2007) is the
33 melt-blending technique with different polymers and/or additives (Frédéric, Sterzel, and
34 Wegner 2014; Gu et al. 2008; Hashima, Nishitsuji, and Inoue, 2010; Jo et al. 2012;
35 Leung et al. 2009; Rohman et al. 2007). Previously (Anakabe et al. 2015, 2016, 2018),
36 different blends of extruded poly(lactic acid)/poly(methyl methacrylate) (PLA/PMMA)
37 were studied. It was observed that after the addition of 3 pph of poly(styrene-co-
38 glycidyl methacrylate) (P(S-co-GMA)) copolymer to PLA/PMMA (80/20 wt%) blend,
39 the elongation at break and impact resistance values improved around 1300 % and 60
40 %, respectively, keeping the tensile strength and modulus values almost similar to
41 PLA/PMMA blend. However, the blend showed a pronounced loss of stiffness around
42 70 °C due to the amorphous microstructure presented. Thus, the incorporation of
43 cellulosic fibers combined with an annealing process is a good approach to increase the
44 Heat Distortion Temperature (HDT). Previously (Orue et al. 2020), it was observed that
45 the estimated HDT value of composites based on PLA/PMMA matrix and sisal fiber
46 bundles without copolymer increased considerable after the annealing process but in
47 detriment to tensile strength value. It was concluded that the thermal treatment damaged
48 the fiber/matrix adhesion and created cracks. Therefore, the use of a compatibilizer
49 agent could be an interesting approach to reduce the damage on the fiber/matrix
50 adhesion and the formation of cracks due to the annealing process.

51 The main aim of this work is to study the effect of annealing process on the properties
52 of composites based on sisal fiber bundles and PLA/PMMA matrix modified with P(S-
53 co-GMA) copolymer. To date, there is not any published research work where
54 PLA/PMMA blend modified with 3 pph of P(S-co-GMA) copolymer was reinforced
55 with natural or synthetic fibers. The thermal properties, mechanical properties and the
56 morphological study of the prepared polymer blend and its composites were carried out
57 by differential scanning calorimetry, dynamic mechanical analysis, tensile test, impact
58 test and scanning electron microscopy. Results obtained in this study suggested that the
59 presence of the copolymer is crucial to form a strong adhesion between the fibers and
60 polymeric matrix and consequently to improve both thermomechanical performance and
61 tensile properties after annealing process.

62

63 **2. Experimental part**

64 **2.1. Materials**

65 PLA was purchased from NatureWorks LLC (Ingeo™ 3051D, $M_n = 106,000$ g/mol;
66 PDI: 1.7; ≈ 4.6 % D-lactate). This grade is designed for injection molding applications
67 being the melt flow index between 10 and 25 g/10 min (2.16 kg load, 210°C). The
68 tensile strength and deformation at break of PLA is 48 MPa and of 2.5%, respectively.
69 PMMA was purchased from Evonik ROM GmbH (PLEXIGLAS® zk5BR, $M_n = 70,000$
70 g/mol; PDI: 2.3). This grade is used for injection molding as well as for extrusion
71 processes being the melt flow index around 4 g/10 min. P(S-co-GMA) copolymer (M_n
72 = 29,000 g/mol; PDI: 1.9) was kindly supplied by Macro-M (Kuo Group). Copolymer
73 composition consisted of 80% styrene and 20% methacrylate, and glycidyl substitution
74 was present at 50% of the methacrylate groups (Anakabe et al. 2016).

75 Sisal, *Agave sisalana*, fiber bundles cultivated in Africa were kindly supplied by
76 Celulosa de Levante S.A. The cellulose content was determined previously being
77 around 62% (Mondragon et al. 2014). To remove non-cellulosic compound from sisal
78 fibers NaOH solution was prepared. Sodium hydroxide pellets, supplied by Panreac,
79 were used to prepare NaOH solution. The alkali treatment of fibers was carried out
80 following the conditions described in a previous work (Orue et al. 2015). After alkali
81 treatment, the cellulose content and the thermal stability of fibers increased due to the
82 extraction of non-cellulosic compounds such as hemicelluloses and lignins. The tensile
83 strength and modulus of alkali treated sisal fibers is 352 MPa and 5 GPa, respectively.
84 (Orue et al. 2015).

85 **2.2. Compounding and processing of materials**

86 Previously dried PLA and PMMA pellets were melt-blended in a HAAKE Rheomix
87 600 internal mixer at 215 °C. Once PLA/PMMA (80/20 wt%) blend was melted, 3 pph
88 of copolymer was added in the internal mixer and the blend was mixed during 5 min at
89 50 rpm after the torque value began to increase. Afterward, dried NaOH treated sisal
90 fibers were added in the internal mixer and they were mixed during 5 min at 50 rpm.
91 The fiber loading varied in the composites from 20 to 40 wt%.

92 All pelletized blends were dried in an oven prior to process by injection molding
93 technique in a HAAKE Minijet II. 63.5 mm length dog bone specimens with a narrow
94 section of $3.18 \times 3.29 \text{ mm}^2$ (ASTM-D638-10, type V) were obtained. The gage length
95 was 10 mm and 1 mm/min test speed was selected. Some tensile specimens were
96 annealed at 105 °C for 15 h.

97 Non-annealed and annealed specimens were characterized by means of different
98 characterization techniques.

99

100 **2.3. Characterization**

101 ***2.3.1. Tensile test***

102 Tensile tests were performed according to ASTM D638 standard using Insight 10
103 testing system. Tensile tests were carried out at 1 mm/min deformation rate and tensile
104 properties were determined.

105

106 ***2.3.2. Unnotched impact test***

107 Unnotched Charpy impact tests were carried out by means of an IMPats-15 impact
108 pendulum with a 2 J hammer with a support span of 40 mm. Even though sample
109 geometry used did not follow any standards, for comparison purposes, injection molded
110 V type specimens were cut to a length of 63.5 mm with a section of 3.18 x 3.29 mm².

111

112 ***2.3.3. Scanning electron microscopy***

113 SEM micrographs were performed by JSM-6400 equipment. Impact fractured surfaces
114 were previously coated with gold using Q150TES metallizer.

115

116 ***2.3.4. Differential scanning calorimetry***

117 Samples were subjected to two heating runs from 0 °C to 180 °C under a nitrogen
118 atmosphere in a Mettler Toledo differential scanning calorimetry (DSC). First heating
119 scan was carried out at 10 °C/min to remove the thermal history of non-annealed
120 samples whereas the second heating scan was taken out at 3 °C/min. For annealed
121 samples, only one heating scan was carried out from 0 °C to 180 °C at 3 °C/min. The
122 crystallinity degree (χ_c) of samples was determined according to Eq. (1):

123
$$\chi_c = \left(\frac{\Delta H_m - \Delta H_{cc}}{\Delta H_{100\%} \times w_{PLA}} \right) \times 100 \quad (1)$$

124 where $\Delta H_{100\%}$ is the melt enthalpy for theoretical 100 % crystalline PLA, ΔH_{cc} is the
125 enthalpy of cold-crystallization process, ΔH_m is the enthalpy of melting process, and
126 w_{PLA} is the weight fraction of PLA. In this work, a value of 93 J/g was taken as the melt
127 enthalpy of 100 % crystalline PLA (Fisher, Sterzel, and Wegner 1973).

128

129 **2.3.5. Dynamic-mechanical analysis**

130 Dynamic-mechanical analysis (DMA) tests of samples were performed in torsion mode
131 at a frequency of 1.6 Hz and 0.005 % strain using an ARES rheometer. The temperature
132 scan was carried out over the temperature range of 30 °C to 150 °C.

133

134 **2.4. Statistical analysis**

135 The statistical analysis was performed using one-way ANOVA in the OriginPro
136 (Version 9.0) software program and Tukey's test was used for multiple comparisons.

137 Differences were statistically significant at $P < 0.05$ level.

138

139 **3. Results and discussion**

140 **3.1. The effect of annealing process on the studied systems properties**

141 **3.1.1 Thermal properties of studied systems**

142 The heating scan thermograms of unreinforced polymer blend and its composites based
143 on 30 wt% sisal fibers before and after annealing process are shown in Figure 1. Before
144 annealing, unreinforced polymer blend and its composite were almost totally amorphous
145 materials showing low crystallinity degree values. After annealing, the glass transition
146 temperature (T_g) of PLA/PMMA blend raised from 57.8 °C to 63.1 °C because of the

147 segmental rearrangement of the PLA chains (Lv et al. 2015), whereas the T_g of
148 composite maintained similar. On the other hand, the crystallinity degree of
149 unreinforced polymer blend increased from 2.1 % to 22.1 % after annealing process
150 while the composites showed an increment up to 37.5 %, suggesting that sisal fibers
151 acted as nucleating agent (Perez-Fonseca et al. 2016; Sarasini et al. 2013; Wang et al.
152 2011). The presence of PMMA polymer hindered the crystallization of PLA polymer
153 (Anakabe et al. 2015), since the obtained crystallinity degree values were lower than
154 those obtained previously for PLA/sisal fibers composites (Orue, Eceiza, and Arbelaz
155 2018).

156 **Insert Figure 1 here**

157 **3.1.2 Thermomechanical properties of studied systems**

158 The variations of the storage modulus, loss modulus and $\tan \delta$ values of unreinforced
159 polymer blend and its composites before and after annealing process are illustrated in
160 Figures 2 and 3, respectively. The storage modulus increased with increasing the fiber
161 content that is in agreement with the trend observed in the literature for other
162 composites based on cellulosic fibers and PLA polymer (Du et al. 2014; Perez-Fonseca
163 et al. 2016). After the annealing process, a reduction on the modulus values was
164 observed around 72 °C. This decrease was related to the amorphous relaxation of PLA
165 and was more gradual in the case of composites rather than on polymer blends.

166

167 **Insert Figure 2 here**

168 **Insert Figure 3 here**

169 Concerning the $\tan \delta$ values, Figures 2c and 3c, annealed systems not only showed
170 slightly higher T_g values than non-annealed counterparts, but also exhibited lower

171 height of $\tan \delta$ suggesting that annealed systems presented lower damping than non-
172 annealed counterparts due to the crystallinity increment. Obtained results confirmed that
173 both the addition of fibers and annealing process contributed to improve the thermo-
174 mechanical behavior of unreinforced polymer blend. The HDT of samples was
175 estimated using the correlation established by Takemori (1979) between the HDT and
176 the temperature at which the Young's modulus equals 0.75 GPa. The Young's modulus,
177 E , was calculated according to Eq. (5).

$$178 \quad E = 2(1 + \nu)\sqrt{(E')^2 + (E'')^2} \quad (5)$$

179 where ν is the Poisson ratio and is assumed to be 0.33 which is typical for glassy
180 polymers such as PLA and PMMA, whereas E' and E'' were the storage and loss
181 modulus, respectively. Table 1 shows that the estimated HDT values markedly
182 increased for unreinforced polymer blend and its composites after the annealing process.
183 Furthermore, it was observed that the increment of estimated HDT value of composites
184 after annealing process was higher with increasing the fiber content. Many research
185 works showed that the annealing process increases the HDT of composites based on
186 PLA polymer matrix (Bubeck et al. 2018; Shi et al. 2012). Previously, the HDT value of
187 commercial neat PLA used in the current work was estimated, being 59.5 °C (Orue et al.
188 2020). Annealed composites with a fiber loading of 40 wt% showed an increment of the
189 estimated heat deflection temperature of around 40 °C respect to commercial neat PLA.

190 **Insert Table 1 here**

191

192 **3.1.3 Mechanical properties of studied systems**

193 Figure 4 a-d shows the tensile and impact properties of unreinforced polymer blend and
194 its composites before and after annealing process. The statistical significance of the

195 results was evaluated by one-way ANOVA. The different letters means that the values
196 are statistically different at 95% significance level. Before the annealing process,
197 unreinforced polymer blend showed the tensile strength and Young's modulus values
198 around 61.5 MPa and 3.2 GPa, respectively, whereas the elongation at break value was
199 137 %. These values that were obtained by mixing the polymers with the copolymer in
200 an internal mixer, were similar to those obtained by twin-screw extrusion (Anakabe et
201 al. 2016). It was observed in Figure 4a that, in general, the tensile strength value of
202 composites increased after the annealing process. The tensile strength values of
203 annealed composites are at least 50 % higher than the strength data of commercial neat
204 PLA used in the current work. One of the reasons of this improvement on the tensile
205 strength values could be the increment observed in the crystallinity of the samples.
206 However, the crystallinity degree increment could not be the unique reason for
207 obtaining higher tensile strength values after annealing process. In this way,
208 biocomposites based on PLA/PMMA matrix without copolymer were studied in a
209 previous work (Orue et al. 2020) and it was observed that although crystallinity degree
210 of composites increased after the annealing process, the tensile strength values
211 decreased due to the damage suffered in the fiber/matrix adhesion. Therefore, it seemed
212 that the presence of copolymer not only improve the interfacial adhesion between the
213 PLA-rich and PMMA-rich dispersed phases (Anakabe et al. 2016), but also improved
214 the adhesion between fibers and polymer matrix.

215 **Insert Figure 4 here**

216 Figure 4b shows that after the annealing process the Young's modulus value of
217 unreinforced polymer blend was similar to non-annealed counterpart. Nevertheless, the
218 modulus value of composites increased after the annealing process being in accordance

219 with results found in the literature for composites based on PLA and cellulosic materials
220 (Bubeck et al. 2018; Perez-Fonseca et al. 2016).

221 In general, as the fiber loading was increased the reported strength and modulus values
222 were different by the one-way analysis of variance test at 95% significance level,
223 observing more clearly this difference in tensile modulus values.

224 The crystallization of PLA resulted in an embrittlement of the unreinforced blend
225 (Figure 4c) and consequently the elongation at break values decreased after the
226 annealing process. Nevertheless, the elongation at break values of annealed composites
227 were similar to non-annealed counterparts. Furthermore, the deformation at break value
228 of annealed composites is slightly higher than the value of commercial neat PLA used
229 in the current work. Figure 4d shows that the impact strength of unreinforced polymer
230 blend increased up to 32 kJ/m² after annealing process. On the other hand, the addition
231 of sisal fibers reduced the impact resistance of PLA/PMMA blend, being the impact
232 strength values of annealed composites similar to non-annealed counterparts. Regarding
233 composite values, the elongation at break and impact strength values of composites are
234 not statistically different at different fiber loading and showed the same letter.

235 Obtained tensile strength values suggested that the addition of copolymer resulted in
236 improved matrix/fiber adhesion. Probably, the residual epoxy groups of P(S-co-GMA)
237 copolymer which did not react with the functional end-groups of PLA could have
238 reacted with the –OH groups in the surface of the fibers creating new covalent bonds
239 (Figure 5).

240 **Insert Figure 5 here**

241 It was previously reported that the torque value started to stabilize after around 5 min of
242 blending (Anakabe et al. 2018), just at the moment when sisal fibers were added to

243 PLA/PMMA-based polymer blend. This fact and obtained tensile strength values
244 suggested that unreacted epoxy groups of copolymer could react with hydroxyl groups
245 of sisal fibers.

246

247 **3.1.4 Morphology of impact fractured surfaces**

248 Figure 6 a-d shows the SEM micrographs of the impact fractured surfaces of
249 unreinforced polymer blend and composite based on 30 wt% sisal fibers before and
250 after annealing process. Comparing the fractured surfaces of unreinforced systems, no
251 significant differences were observed before and after annealing process. In SEM
252 micrographs of composites, Figure 6b and d, split sisal fibers can be observed
253 suggesting that upon debonding, energy dissipation occurs along the fiber prior to pull-
254 out (Haameem et al, 2016; Wong et al. 2010). The addition of the copolymer increased
255 considerably the viscosity of the blend in the internal mixer (Anakabe et al. 2016) and
256 consequently, high shear stresses could split the sisal fibers which were fibrillated
257 during the alkali treatment. The splitting of sisal fibers could increase the capacity to
258 dissipate the energy during the impact test. This fact, together with the improved
259 adhesion between the fiber and polymer matrix, could be the reasons for obtaining
260 impact strength values slightly higher than the values reported in the previous work for
261 composites based on PLA/PMMA matrix and sisal fibers without copolymer (Orue et
262 al. 2020). Taking into account the tensile and impact properties, as well as the
263 micrographs of the fractured surface, the shrinkage of PLA polymer caused during the
264 annealing process seemed to damage to a lesser extent the matrix/fiber adhesion in
265 systems with copolymer than in composites without copolymer that were studied
266 previously (Orue et al. 2020).

267 **Insert Figure 6 here**

268

269 **4. Conclusions**

270 The incorporation of cellulosic fibers combined with an annealing process in the
271 presence of a copolymer that can react chemically with matrix and fiber is an effective
272 approach to improve the thermomechanical performance and the tensile properties of
273 composites based on sisal fiber bundles and poly(lactic acid)/poly(methyl methacrylate)
274 matrix. Results obtained in the current study suggested that the presence of the
275 copolymer is crucial to form a strong adhesion between the fibers and polymeric matrix
276 and consequently to improve both thermomechanical performance and tensile properties
277 after annealing process. It must highlight that the estimated heat deflection temperature
278 (HDT) of annealed composite with 40 wt% of fiber increased around 40 °C respect to
279 commercial neat PLA and the tensile strength value increased around 50% respect to
280 commercial neat PLA.

281

282 **References**

- 283 Arbelaiz, A., U. Txueka, I. Mezo, and A. Orue. 2020. Biocomposites Based on
284 Poly(Lactic Acid) Matrix and Reinforced with Lignocellulosic Fibers: The Effect of
285 Fiber Type and Matrix Modification. *Journal of Natural Fibers*.
286 doi:10.1080/15440478.2020.1726247
- 287 Anakabe, J., A. M. Zaldua-Huici, A. Eceiza, and A. Arbelaiz. 2015. Melt blending of
288 polylactide and poly(methyl methacrylate): Thermal and mechanical properties and
289 phase morphology characterization. *Journal of Applied Polymer Science* 132 (42677):1-
290 8. doi:10.1002/app.42677

291 Anakabe J., A. M. Zaldua-Huici, A. Eceiza, and A. Arbelaiz. 2016. The effect of the
292 addition of poly(styrene-co-glycidyl methacrylate) copolymer on the properties of
293 polylactide/poly(methyl methacrylate) blend. *Journal of Applied Polymer Science* 133
294 (43935):1-10. doi:10.1002/app.43935

295 Anakabe J., A. Orue, A. M. Zaldua-Huici, A. Eceiza, and A. Arbelaiz. 2018. Properties
296 of PLA/PMMA blends with high polylactide content prepared by reactive mixing in
297 presence of poly(styrene-co-glycidyl methacrylate) copolymer. *Journal of Applied*
298 *Polymer Science* 135 (46825):1-7. doi:10.1002/app.46825

299 Auras R., B. Harte, and S. Selke. 2004. An overview of polylactides as packaging
300 materials. *Macromolecules Bioscience* 4:835-64. doi:10.1002/mabi.200400043

301 Bosquetti M., A. L. da Silva, E. C. Azevedo, and L. F. Berti. 2019. Analysis of the
302 Mechanical Strength of Polymeric Composites Reinforced with Sisal Fibers. *Journal of*
303 *Natural Fibers*. doi:10.1080/15440478.2020.1726247

304 Bubeck R. A., A. Merrington, A. Dumitrascu, and P. B. Smith. 2018. Thermal analyses
305 of poly(lactic acid) PLA and micro-ground paper blends. *Journal of Thermal Analysis*
306 *and Calorimetry* 131 (1):309-316. doi:10.1007/s10973-017-6466-2

307 Du Y., T. Wu, N. Yan, M. T. Kortschot, and R. Farnood. 2014. Fabrication and
308 characterization of fully biodegradable natural fiber-reinforced poly (lactic acid)
309 composites. *Composites, Part B: Engineering* 56:717-723.
310 doi:10.1016/j.compositesb.2013.09.012

311 Fisher E. W., H. J. Sterzel, and G. Wegner. 1973. Investigation on the structure of
312 solution grown crystals of lactide copolymers by mean of chemical reactions. *Kolloid*
313 *Zeitschrift & Zeitschrift fuer Polymere* 251 (11):980-990. doi:10.1007/BF01498927

314 Frédéric B., T. Samira, and T. Mohamed. 2014. Graft copolymers of poly(methyl
315 methacrylate) and poly(lactic acid) or poly(3-hydroxybutyrate): Synthesis by reactive
316 extrusion and characterization. *Macromolecular Reaction Engineering* 8 (2):149-59.
317 doi:10.1002/mren.201300128

318 Gu S, Y., K. Zhang, J. Ren, and H. Zhan. 2008. Melt rheology of
319 polylactide/poly(butylene adipate-co-terephthalate) blends. *Carbohydrate Polymers* 74
320 (1):79-85. doi:10.1016/j.carbpol.2008.01.017

321 Haameem M., M. S. A. Majid, M. Afendi, H. F. A. Marzuki, I. Fahmi, and A. G.
322 Gibson. 2016. Mechanical properties of Napier grass fibre/polyester composites.
323 *Composite Structures* 136:1-10. doi:10.1016/j.compstruct.2015.09.051

324 Hashima K., S. Nishitsuji, and T. Inoue. 2010. Structure properties of super-tough PLA
325 alloy with excellent heat resistance. *Polymer* 51 (17):3934-39.
326 doi:10.1016/j.polymer.2010.06.045

327 Jo M. Y., Y. J. Ryu, J. H. Ko, and J. S. Yoon. 2012. Effects of compatibilizers on the
328 mechanical properties of ABS/PLA composites. *Journal of Applied Polymer Science*
329 125 (S2):E231-E238. doi:10.1002/app.36732

330 Kale G., R. Auras, S. P. Singh, and R. Narayan. 2007. Biodegradability of polylactide
331 bottles in real and simulated composting conditions. *Polymer Testing* 26 (8):1049-1061.
332 doi:10.1016/j.polymertesting.2007.07.006

333 Leung B. O., A. P. Hitchcock, J. L. Brash, A. Scholl, and A. Doran. 2009. Phase
334 segregation in polystyrene-polylactide blends. *Macromolecules* 42 (5):1679-84.
335 doi:10.1021/ma802176b

336 Lv S., J. Gu, J. Cao, H. Tan, and Y. Zhang. 2015. Effect of annealing on the thermal
337 properties of poly(lactic acid)/starch blends. *International Journal of Biological*
338 *Macromolecules* 74:297-303. doi:10.1016/j.ijbiomac.2014.12.022

339 Mondragon G., S. Fernandes, A. Retegi, C. Pena, I. Algar, A. Eceiza, and A. Arbelaiz.
340 2014. A common strategy to extracting cellulose nanoentities from different plants.
341 *Industrial Crops and Products* 55:140-148. doi:10.1016/j.indcrop.2014.02.014

342 Orue A., A. Jauregi, C. Peña-Rodríguez, J. Labidi, A. Eceiza, and A. Arbelaiz. 2015.
343 The effect of surface modifications on sisal fiber properties and sisal/poly(lactic acid)
344 interface adhesion. *Composites, Part B: Engineering* 73:132-138.
345 doi:10.1016/j.compositesb.2014.12.022

346 Orue A, Jauregi A, Unsuain U, Labidi J, Eceiza A, Arbelaiz A. 2016. The effect of
347 alkaline and silane treatments on mechanical properties and breakage of sisal fibers and
348 poly(lactic acid)/sisal fiber composites. *Composites, Part A: Applied Science and*
349 *Manufacturing* 84:186-195. DOI:10.1016/j.compositesa.2016.01.021

350 Orue A., A. Eceiza, and A. Arbelaiz. 2018. The effect of fiber surface treatments,
351 plasticizer addition and annealing process on the crystallization and the thermo-
352 mechanical properties of poly(lactic acid) composites. *Industrial Crops and Products*
353 118:321-333. doi:10.1016/j.indcrop.2018.03.068

354 Orue A., J. Anakabe, A. M. Zaldua-Huici, A. Eceiza, and A. Arbelaiz. 2020.
355 Preparation and characterization of composites based on poly(lactic acid)/poly(methyl
356 methacrylate) matrix and sisal fibers: comparison study with other thermoplastic
357 composites. *Journal of Thermoplastic Composite Materials*.
358 doi:10.1177/0892705720930780

359 Perez-Fonseca A. A., J. R. Robledo, R. Gonzalez, and D. Rodrigue. 2016. Effect of
360 thermal annealing on the mechanical and thermal properties of polylactic acid-cellulosic
361 fiber biocomposites. *Journal of Applied Polymer Science* 133 (31):1-9.
362 doi:10.1002/app.43750

363 Rohman G., F. Lauprêtre, S. Boileau, P. Guérin, and D. Grande. 2007. Poly(D,L-
364 lactide)/poly(methyl methacrylate) interpenetrating polymer networks: Synthesis,
365 characterization, and use as precursors to porous polymeric materials. *Polymer* 48:7017-
366 7028. doi:10.1016/j.polymer.2007.09.044

367 Sarasini F., D. Puglia, E. Fortunati, J. M. Kenny, and C. Santulli. 2013. Effect of fiber
368 surface treatments on thermo-mechanical behavior of poly(lactic acid)/phormium tenax
369 composites. *Journal of Polymers and the Environment* 21 (3):881–891.
370 doi:10.1007/s10924-013-0594-y

371 Shi Q. F., H. Y. Mou, Q. Y. Li, J. K. Wang, and W. H. Guo. 2012. Influence of heat
372 treatments on the heat distortion temperature of poly(lactic acid)/bamboo fiber/talc
373 hybrid biocomposites. *Journal of Applied Polymer Science* 123 (5):2828-2836.
374 doi:10.1002/app.34807

375 Takemori M.T. 1979. Towards an understanding of the heat distortion temperature of
376 thermoplastics. *Polymer Engineering and Science* 19 (15):1104-1109.
377 doi:10.1002/pen.760191507

378 Wang Y., B. Tong, S. Hou, M. Li, and C. Shen. 2011. Transcrystallization behavior at
379 the poly(lactic acid)/sisal fibre biocomposite interface. *Composites, Part A: Applied*
380 *Science and Manufacturing* 42 (1):66-74. doi:10.1016/j.compositesa.2010.10.006

381 Wong K. J., S. Zahi, K.O. Low, and C. C. Lim. 2010. Fracture characterization of short
382 bamboo fibre reinforced polyester composites. *Materials & Design* 31 (9):4147-4154.
383 doi:10.1016/j.matdes.2010.04.029

384 Zhao X., Z. Sun, and A. Tang. 2020. Effects of Hyperbranched Polyamide on the
385 Properties of Sisal Fiber Reinforced Polypropylene Composites, *Journal of Natural*
386 *Fibers*. doi: 10.1080/15440478.2020.1787923

387 Zhu Z., M. Hao, and N. Zhang. 2020. Influence of contents of chemical compositions
388 on the mechanical property of sisal fibers and sisal fibers reinforced PLA composites,
389 *Journal of Natural Fibers* 17 (1):101-112. doi: 10.1080/15440478.2018.1469452

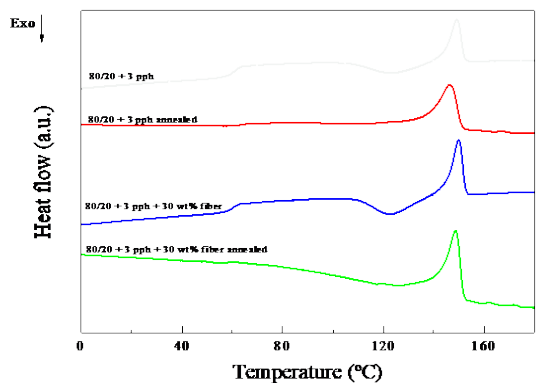


Figure 1.

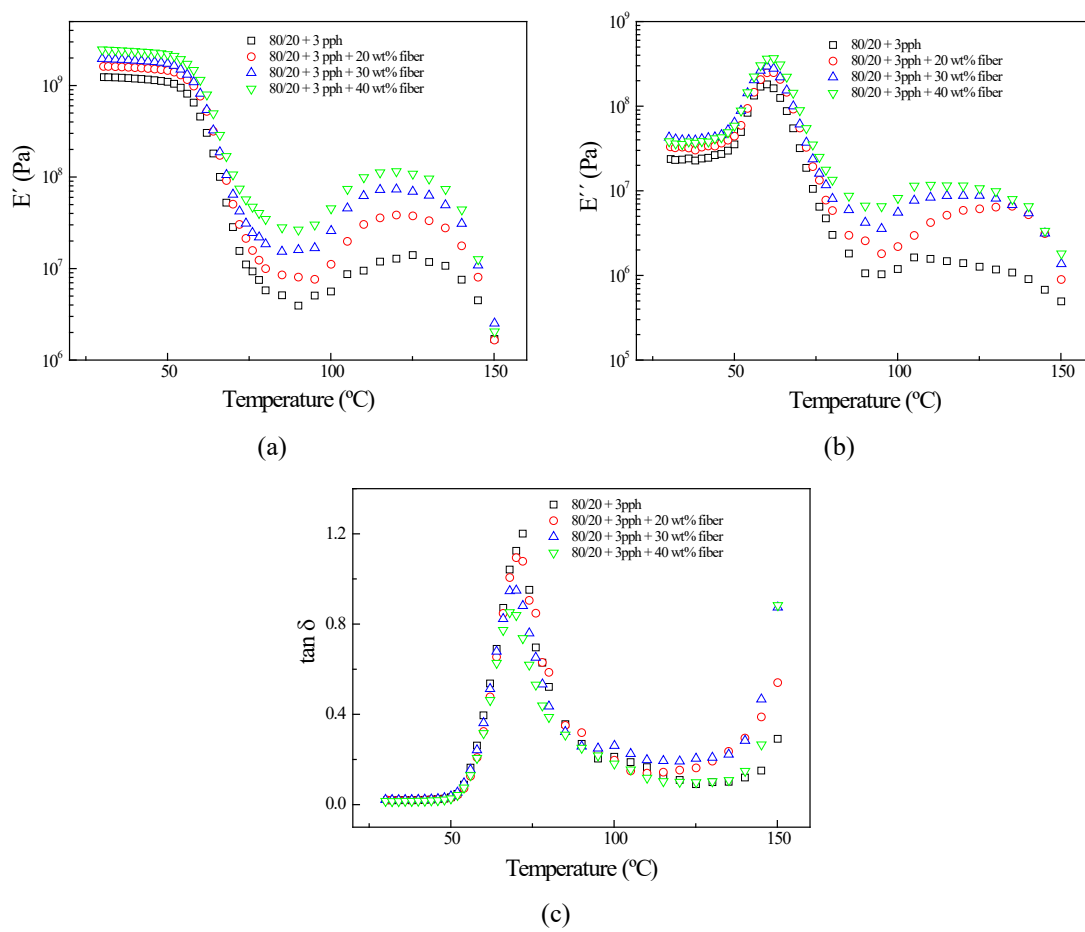


Figure 2.

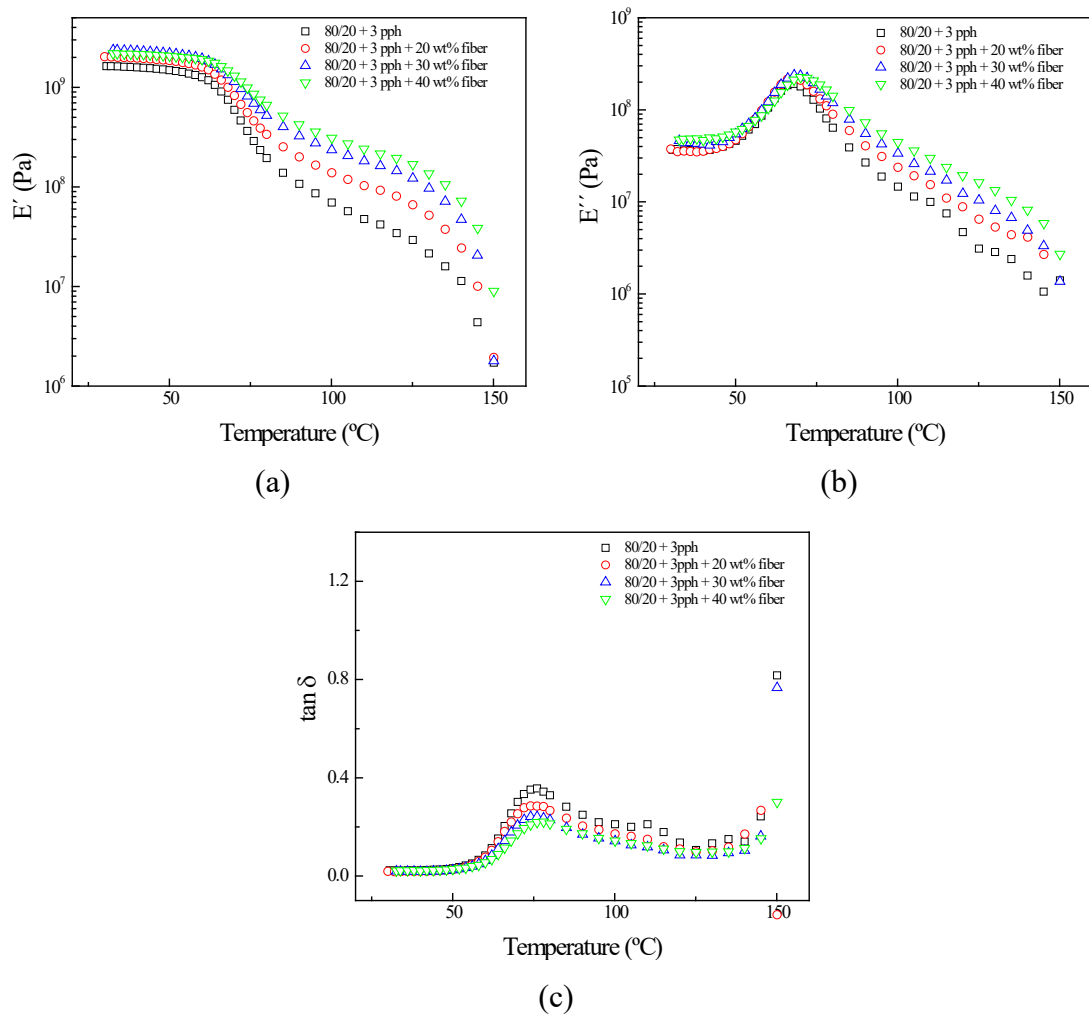


Figure 3.

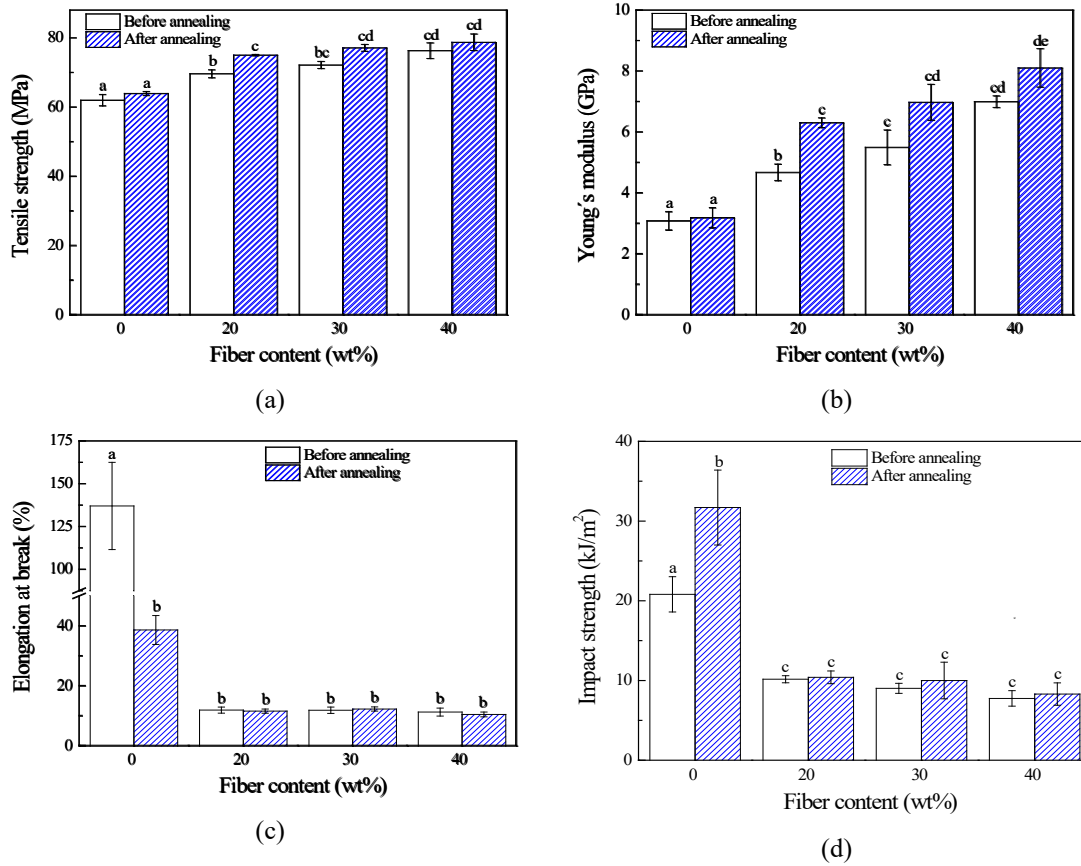


Figure 4.

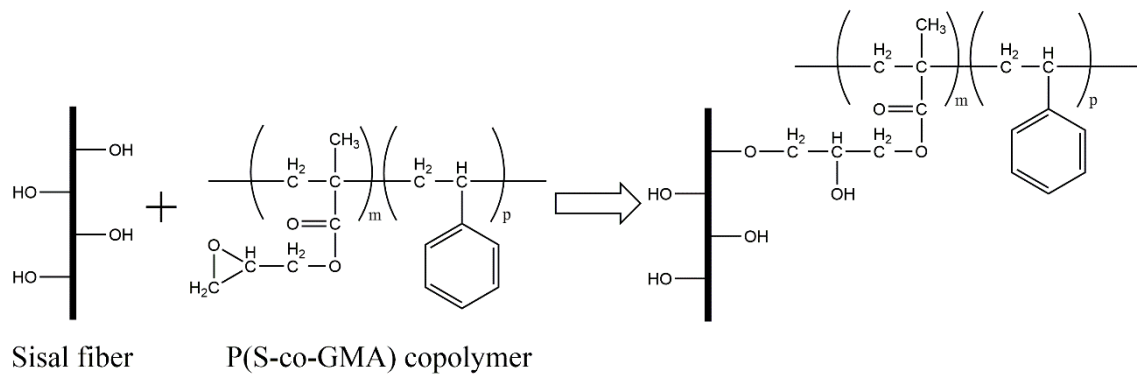
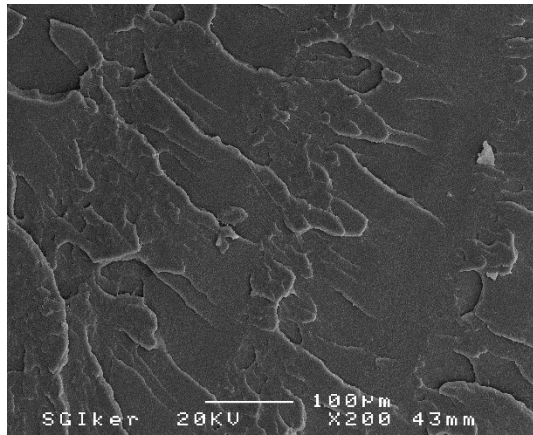
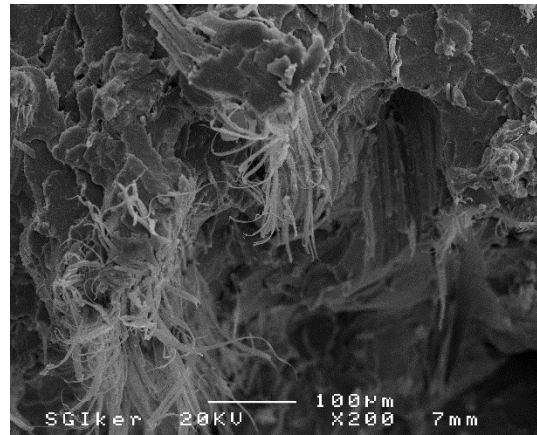


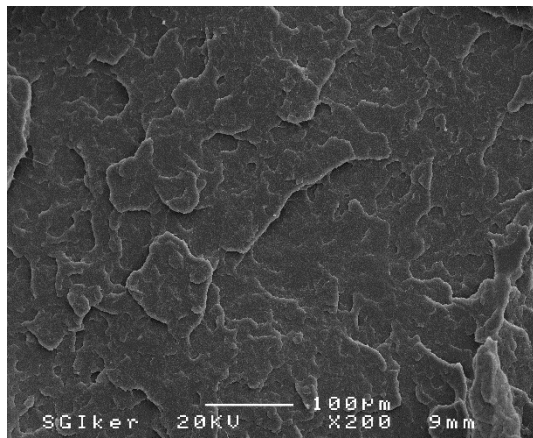
Figure 5.



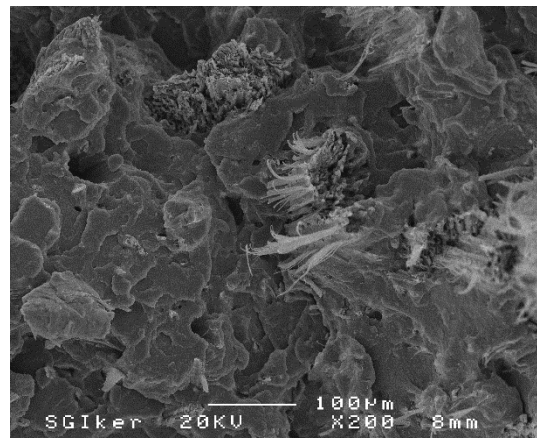
(a)



(b)



(c)



(d)

Figure 6.

Table 1

System	HDT (°C)		
	Before	After	Increment
80/20 + 3 pph	63.0	76.9	13.9
80/20 + 3 pph + 20 wt% fiber	65.3	83.8	18.5
80/20 + 3 pph + 30 wt% fiber	65.5	94.8	29.4
80/20 + 3 pph + 40 wt% fiber	67.2	104.1	36.9